

## Ambient condition laser writing of graphene structures on polycrystalline SiC thin film deposited on Si wafer

Naili Yue, Yong Zhang, and Raphael Tsu

Citation: *Appl. Phys. Lett.* **102**, 071912 (2013); doi: 10.1063/1.4793520

View online: <http://dx.doi.org/10.1063/1.4793520>

View Table of Contents: <http://apl.aip.org/resource/1/APPLAB/v102/i7>

Published by the [American Institute of Physics](#).

---

### Related Articles

Photoluminescence studies in CuInS<sub>2</sub> thin films grown by sulfurization using ditertiarybutylsulfide  
*J. Appl. Phys.* **112**, 123521 (2012)

Dielectric function spectra at 40K and critical-point energies for CuIn<sub>0.7</sub>Ga<sub>0.3</sub>Se<sub>2</sub>  
*Appl. Phys. Lett.* **101**, 261903 (2012)

Composition dependent metal-semiconductor transition in transparent and conductive La-doped BaSnO<sub>3</sub> epitaxial films  
*Appl. Phys. Lett.* **101**, 241901 (2012)

Valley polarization and intervalley scattering in monolayer MoS<sub>2</sub>  
*Appl. Phys. Lett.* **101**, 221907 (2012)

Second order nonlinear optical properties of AIBIIIC<sub>2</sub>VI chalcopyrite semiconductors  
*Appl. Phys. Lett.* **101**, 192105 (2012)

---

### Additional information on *Appl. Phys. Lett.*

Journal Homepage: <http://apl.aip.org/>

Journal Information: [http://apl.aip.org/about/about\\_the\\_journal](http://apl.aip.org/about/about_the_journal)

Top downloads: [http://apl.aip.org/features/most\\_downloaded](http://apl.aip.org/features/most_downloaded)

Information for Authors: <http://apl.aip.org/authors>

## ADVERTISEMENT

**AIP** | Applied Physics  
Letters

**EXPLORE WHAT'S NEW IN APL**

**SUBMIT YOUR PAPER NOW!**

**SURFACES AND INTERFACES**  
Focusing on physical, chemical, biological, structural, optical, magnetic and electrical properties of surfaces and interfaces, and more...

**ENERGY CONVERSION AND STORAGE**  
Focusing on all aspects of static and dynamic energy conversion, energy storage, photovoltaics, solar fuels, batteries, capacitors, thermoelectrics, and more...

## Ambient condition laser writing of graphene structures on polycrystalline SiC thin film deposited on Si wafer

Naili Yue, Yong Zhang,<sup>a)</sup> and Raphael Tsu

*Department of Electrical and Computer Engineering and The Center for Optoelectronics and Optical Communications, The University of North Carolina at Charlotte, Charlotte, North Carolina 28223, USA*

(Received 11 January 2013; accepted 12 February 2013; published online 22 February 2013)

We report laser induced local conversion of polycrystalline SiC thin-films grown on Si wafers into multi-layer graphene, a process compatible with the Si based microelectronic technologies. The conversion can be achieved using a 532 nm CW laser with as little as 10 mW power, yielding  $\sim 1 \mu\text{m}$  graphene discs without any mask. The conversion conditions are found to vary with the crystallinity of the film. More interestingly, the internal structure of the graphene disc, probed by Raman imaging, can be tuned with varying the film and illumination parameters, resembling either the fundamental or doughnut mode of a laser beam. © 2013 American Institute of Physics. [<http://dx.doi.org/10.1063/1.4793520>]

Mechanically exfoliated graphene has served very well the purpose of fundamental study of this unique material.<sup>1</sup> Various growth techniques have been revisited and developed to obtain single- or few-layer graphene and patterned graphene structures in a more viable way for device applications.<sup>1–7</sup> These options also provide the opportunities to explore a variety of graphene based materials and structures that might be able to offer interesting properties beyond those intrinsic to a single layer graphene. For the device application, a top-down approach is often adopted, i.e., using lithographic methods to define and produce graphene features of desirable size, shape, and density starting from a large graphene sheet on a substrate either through transfer or direct deposition; a typical bottom-up approach would be to first pattern a substrate (e.g., with nickel) followed by the selective graphene deposition. We recently demonstrated the feasibility of an alternative bottom-up approach for making graphene micro- and nano-structures, that is, laser induced local conversion (LILC) of a SiC thin-film into multilayer graphene (MLG).<sup>8</sup> Specifically, optical diffraction limit size graphene structures (e.g., in the order of  $\mu\text{m}$  in visible wavelength) can be directly written on a Si wafer size SiC thin film using a tightly focused laser beam with a high numerical aperture (NA) microscope lens, and pre- or post- growth patterning can in-principle achieve even smaller feature sizes down to 100 nm.<sup>8</sup> There have been a number of attempts generating MLG or graphitic structures using laser.<sup>8–13</sup> However, in most cases, only macroscopic graphene structures were produced, except in our preliminary report of direct laser writing<sup>8</sup> and with the help of ion-patterning<sup>10</sup> where a few  $\mu\text{m}$  width graphene ribbons were obtained. Most attempts used single crystalline (4H or 6H) SiC substrates, which typically requires a relatively high power density for conversion. For instance, with a pulsed UV laser, a single crystalline sample required a peak power density  $\sim 6 \times 10^7 \text{ W/cm}^2$  (1.4 J/cm<sup>2</sup> and 25 ns pulse width), whereas ion implantation induced disordering in SiC reduced the threshold power to  $\sim 4 \times 10^6 \text{ W/cm}^2$ .<sup>10</sup> In our approach, because of using polycrystalline SiC thin-films and a high

NA lens, as little as 10 mW power of a 532 nm CW laser, corresponding to  $\sim 2 \times 10^6 \text{ W/cm}^2$ , is sufficient for achieving the conversion. Furthermore, we deposit the SiC film on a Si wafer (3" size currently used), which removes the limitations of the available SiC single crystal size and the associated high cost. More significantly, the process becomes compatible and can be integrated with the Si based microelectronic technologies. The major potential advantages of the LILC over the better developed SiC-to-graphene conversion via thermal sublimation of Si at high temperature ( $>1200 \text{ }^\circ\text{C}$ ) in ultra-high vacuum (UHV)<sup>5</sup> lies in these two aspects: (1) performed at room temperature and in air, and (2) much easier to achieve the spatial selectivity. Other laser assisted graphene deposition techniques have also been reported and are capable of generating 10–20  $\mu\text{m}$  size graphene structures, for instance, on nickel foil in CH<sub>4</sub> and H<sub>2</sub> environment,<sup>14</sup> and on PMMA coated Si wafer,<sup>15</sup> typically carried out in a vacuum chamber using a high power laser (e.g., 3–5 W at 532 nm).

The graphene layers produced by the LILC on SiC have not been demonstrated with good electronic transport, therefore, might not be suited for the electronics without further improvement. However, they can be readily used in various other applications, such as capacitors,<sup>11</sup> bio-sensors,<sup>16</sup> and photonic structures,<sup>17</sup> where high electronic conductivity is not critical or even required. Graphene based photonic structures have recently received considerable interest.<sup>17–19</sup> To tune the working frequency into and explore other photonic applications in optical region, the graphene structure sizes need to be reduced to perhaps the order of 100 nm. The LILC process in conjunction with e-beam patterning could be a viable option. Therefore, the approach reported here could be applicable for fabricating graphene based photonic structures from THz to optical frequencies on a Si wafer size SiC thin-film.

In this Letter, we report (1) the growth control on the grain structure of the SiC film, yielding SiC templates that are appropriate for different conversion conditions (e.g., power density, illumination time) and thus can lead to different photonic elements; (2) the demonstration of  $\sim 1 \mu\text{m}$  size photonic elements exhibiting different internal features by direct laser illumination (i.e., without any patterning); (3) the

<sup>a)</sup>yong.zhang@uncc.edu.

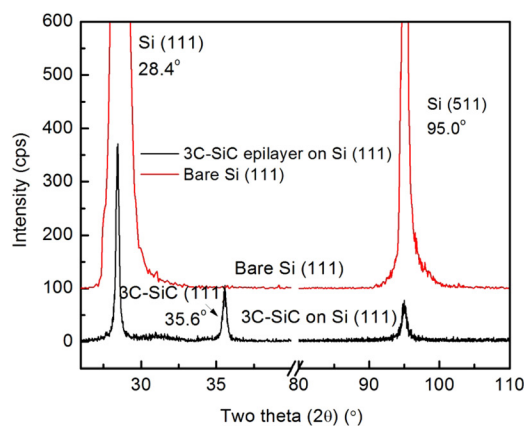
selective growth of SiC micro- and nano-structures on Si wafer, and the subsequent conversion into graphene layers.

An ultrahigh vacuum MBE system (with  $\sim 10^{-10}$  Torr base pressure) is used to grow SiC thin films on Si substrates. Fullerene (C60) powders were used as carbon source. C60 is known to decompose when incident on the Si substrate then react with Si from the substrate to form SiC, under an appropriate combination of substrate temperature ( $T_S$ ) and C60 temperature ( $T_C$ ).<sup>20,21</sup> The typical temperature ranges are  $T_S = 700\text{--}800^\circ\text{C}$  and  $T_C = 500\text{--}600^\circ\text{C}$ , respectively. The optimal combination was found to be  $T_S = 800^\circ\text{C}$  and  $T_C = 550^\circ\text{C}$  for the consideration of crystallinity and uniformity. During growth, the gas or vapor in the chamber was monitored with mass spectrometer, and the film surface quality was inspected with reflection high-energy electron diffraction (RHEED). After 10 min growth, the samples were held at the growth temperature for 5–10 min to homogenize the epitaxial film. Then, the film was allowed to cool down slowly ( $10^\circ\text{C}/\text{min.}$ ) to room temperature. Substrates of three orientations, (100), (110), and (111), were used and grown on simultaneously. They were cleaned to remove surface contaminations and native oxide layer. The substrates were heated up to  $850^\circ\text{C}$  and stayed for half an hour to further remove the residual oxide. Only the results of the (111) substrate are reported here. The surface morphologies and microstructures of SiC thin film were characterized with SEM and XRD. The samples were illuminated with a CW 532 nm laser focused by the microscope of Horiba LabRam HR  $\mu$ -Raman system with a  $100\times$  lens ( $\text{NA} = 0.9$ ). The diffraction limit spot size is  $1.22 \lambda/\text{NA} \approx 0.7 \mu\text{m}$ , corresponding to a power density of  $\sim 2.5 \times 10^6 \text{ W}/\text{cm}^2$  with 10 mW power. The maximum power used is  $\sim 30\text{mW}$ . The illumination

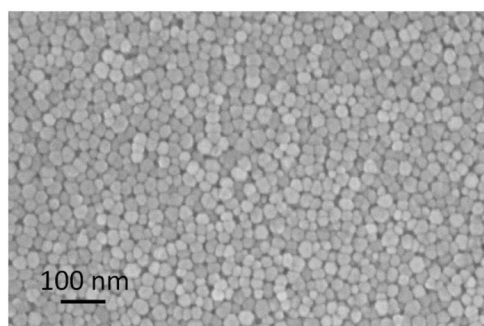
time is controlled by a shutter (SRS 474, Stanford Research System). The shortest shutter opening time is 4 ms. The laser-induced graphene structures were characterized with SEM, TEM, and  $\mu$ -Raman.

Figure 1 shows the basic structural characterization of the as-grown SiC thin-film on the (111) Si substrate: Fig. 1(a) for a typical XRD  $2\theta$  scan of the SiC thin-film with comparison to the substrate; Figs. 1(b) and 1(c) for surface morphology and cross-sectional SEM images, respectively. In Fig. 1(a), an extra XRD peak appears at  $35.56^\circ$ , close to that of the (111) peak of 3C-SiC single crystal at  $35.60^\circ$ , which suggests that the epilayer is 3C-SiC with slight in-plane compressive strain, and the film is highly oriented. Figs. 1(b) and 1(c) show the grain sizes of 20–30 nm and thickness of  $\sim 190 \text{ nm}$ , respectively.

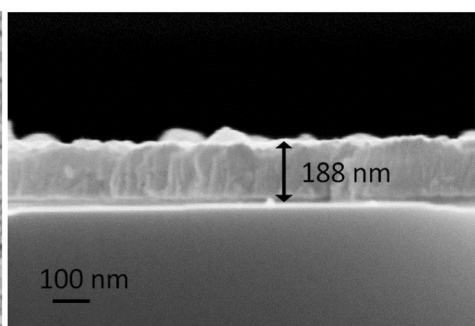
Figure 2 compares the Raman spectra of Si substrate, as-grown SiC film, laser illuminated spot on the SiC film, and C60 powders. Compared to the Si reference that shows the second order Raman features between  $750\text{--}1000 \text{ cm}^{-1}$ ,<sup>22</sup> the as-grown film shows additional Raman features at  $769$  and  $795 \text{ cm}^{-1}$  that can be attributed to 6H-SiC and 3C-SiC,<sup>23</sup> respectively; the illuminated spot exhibits five extra Raman peaks: three prominent ones at  $1352$ ,  $1583$ , and  $2684 \text{ cm}^{-1}$ , and two weaker ones at  $2451$  and  $2927 \text{ cm}^{-1}$ . They are close to, respectively, the well-known Raman features in graphene:<sup>24</sup> the D ( $1350 \text{ cm}^{-1}$ ), G ( $1580 \text{ cm}^{-1}$ ), and 2D ( $2700 \text{ cm}^{-1}$ ) for the first three, T + G ( $2450 \text{ cm}^{-1}$ ) and D + G ( $2928 \text{ cm}^{-1}$ ) for the other two, indicating unambiguously the presence of a MLG or some sort of graphitic structure. Sometimes in the literature, the observation of the D and G peaks alone without the 2D peak was used as evidence for the existence of graphene layers.<sup>25</sup> In fact, as shown in



(a)



(b)



(c)

FIG. 1. XRD spectra and SEM micrographs of a 3C-SiC thin film grown on Si (111): (a) XRD spectra, (b) surface morphology, and (c) cross-section image.

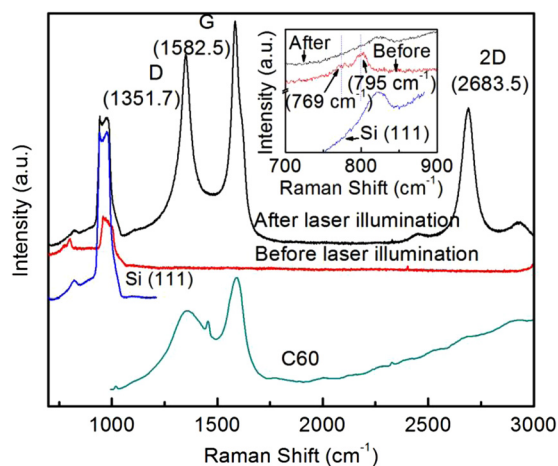
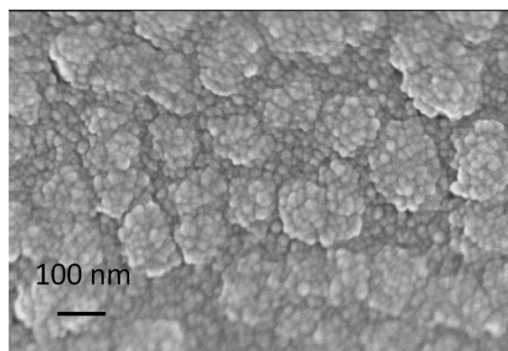


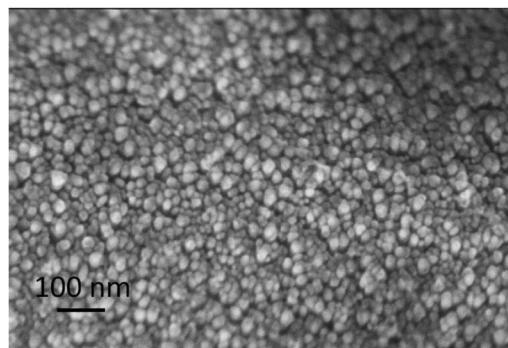
FIG. 2. Raman spectra of as-grown 3C-SiC on Si (111), laser-illuminated spot on 3C-SiC on Si (111), bare Si (111), and C<sub>60</sub> powders. Inset shows the enlarged spectral region of the SiC phonons.

Fig. 2, C<sub>60</sub> powder may also give rise to the D and G peaks, but without the 2D peak, which excludes the possibility that the 2D peak in the spectrum of laser-illuminated 3C-SiC is from C<sub>60</sub>. Based on the fact 2D/G ratio < 1, the laser-induced graphene is likely MLG.<sup>26</sup> The symmetric shape of the 2D peak indicates that the stacking order of graphene layers is turbostratic (i.e., A-A) rather than Bernal stacking (i.e., A-B).<sup>27</sup> The turbostratic stacking is also supported by the TEM image taken from a flake of the material scratched off the sample.<sup>8</sup> The inter-layer spacing was measured to be about 3.70 Å, and the total number of graphene layers is about 8~9 layers. The layer spacing is larger than that of the crystalline graphite with A-B stacking ( $c/2 = 3.35$  Å),<sup>27</sup> but rather close to that of the theoretically predicted A-A stacking graphite of 3.61 Å (0 K).<sup>28</sup> The occasional appearance of the 6H-SiC Raman peak at  $769\text{ cm}^{-1}$  in the as-grown SiC indicates that the SiC film is not in pure 3C phase. As shown in the inset of Fig. 2, both SiC TO peaks diminish after laser illumination, indicating the conversion. Note that because the SiC film is rather thin to begin with, the second order SiC phonon peaks are not visible in our sample, in contrast to virtually all the cases of using a SiC single crystal where the second order SiC phonon peaks interference strongly with the graphene D and G peaks.<sup>12,13</sup>

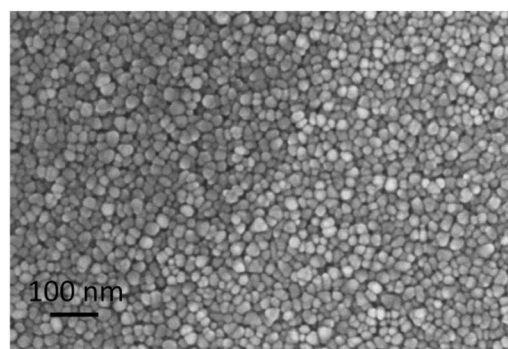
We find that the surface morphology of the SiC film is rather sensitive to the details of the growth procedure. For instance, by adopting different substrate cleaning processes, we obtained three different films with their surface morphologies shown in Figure 3. The substrate of sample A was cleaned with only acetone and methanol, so there might be a few nanometers thick native oxide left on the substrate; sample B with wet-etching (buffered oxide etching), and sample C with reactive ion etching (RIE). The average grain size increases from A to B to C, so does the film uniformity. Sample A shows ~100 nm size domain consisting of small grains and rough surface, which could result from the presence of a thin native oxide layer. The average grain size, uniformity, and surface flatness of sample B is between samples A and C, whereas sample C is most uniform in terms of grain size and surface morphology. Samples A and B have nearly the same thickness of ~190 nm and sample C is ~50 nm



(a)



(b)



(c)

FIG. 3. SEM micrographs of 3C-SiC grown on Si (111): (a) sample A, (b) sample B, and (c) sample C.

thick. Sample C was grown on a SiO<sub>2</sub> patterned Si substrate with ~5 μm wide exposed Si strips. SiC thin-film is found to deposit selectively on the exposed Si area. Due to the shadowing effect of the SiO<sub>2</sub> masks, the SiC film is thinner for the same growth time. With this selective growth, the narrowest SiC ribbons that have been grown are slightly below 90 nm, although the SiC-to-graphene conversion has not yet been demonstrated due to inadequate laser power density illuminating the small width.

Interestingly, these three films exhibit different laser power thresholds and minimum illumination times for the conversion: 10 mW/4 ms (limited by the shortest shutter time available), 17 mW/6 ms, and 22 mW/8 ms, respectively. An optimal combination can be found for a given power level: an illumination time yields maximum 2D peak intensity. The variation in the threshold conditions is likely due to the variation of the thermal conductivity with the crystallinity and thus the local heating temperature: lower thermal

conductivity for a smaller grain size leading to higher local temperature. For sample C, the higher threshold power could also be due to less light absorption of the thinner SiC film. More interestingly, we have found that the internal structures of the converted regions are rather different, as revealed in the SEM images and  $\mu$ -Raman mapping results shown in Figure 4 for the single spot conversion, the creation of a graphene disc, under the optimal conditions 10 mW/4 ms, 17 mW/1 s, and 22 mW/1 s, respectively. The SEM images indicate that the material at the illuminated site is ablated slightly by the laser. The uniformity of the ablated area is quite different for each case, with the illuminated area on sample A being most uniform and the smallest, in contrast to the fact that the surface morphology of sample A is least uniform and the sample shows the lowest crystallinity. It is evident that the feature size on sample B is somewhat larger than that on sample A, presumably due to the higher laser power used associated with the larger average grain size of sample B. The difference between samples B and C could be due to the difference in the average grain size as well as the thickness of the SiC films, which could affect the heat diffusion in the film. The Raman image of sample A, Fig. 4(a), indicates the formation of a graphene disc of comparable size of the ablated area, slightly larger than the laser spot size due to lateral heat diffusion. The intensity profile resembles the fundamental mode of a laser beam, suggesting that the graphene distribution more or less follows that of the

laser intensity with a Gaussian profile. However, the Raman image of sample C, Fig. 4(c), instead resembles a laser doughnut mode or graphene ring, which appears to correlate with the corresponding SEM image showing more ablation near the center of the illuminated spot. The shape of the Raman image of sample B, Fig. 4(b), appears to be between the other two, and the Raman image size is larger as does the ablated area than those of the other two samples. Note that Fig. 4(a) represents the smallest feature,  $\sim 1 \mu\text{m}$ , achieved so far with laser illumination, which likely benefits from the low laser power used associated with the low crystallinity of the film. The conversion mechanism is rather complex, depending on the power density, illumination time, thermal conductivity of the film as well as that of the substrate, and even the environment.<sup>12</sup> Clearly, the epitaxial film provides additional flexibility in controlling the LILC process compared to the use of single crystalline SiC. One may envision producing photonic structures of an array of the components similar to those shown in Fig. 4 and even combinations of the different types of Fig. 4 by either controlling the illumination or growth conditions. Note that with our approaches, the graphene components are already embedded in a dielectric medium either SiC or SiO<sub>2</sub>, which is a desirable situation for making a photonic structure.

In summary, we have shown that the growth of thin-film SiC on a large Si substrate offers greater flexibility for performing laser LILC into graphene layers, and compatibility with the existing Si based micro-electronics and photonics. The LILC process demonstrated here could be further developed into an efficient way to pattern graphene based micro- or nano-structure arrays for applications, such as photonics and bio or chemical sensing.

The research was supported by ARO (Grant No. W911NF-10-1-0281 and monitored by Dr. Pani Varanasi), Charlotte Research Institute, and Northrop Grumman Corp. Y.Z. thanks the support of the Bissell Distinguished Professorship. We thank J. Hudak and J. C. Li for assistance in MBE growth.

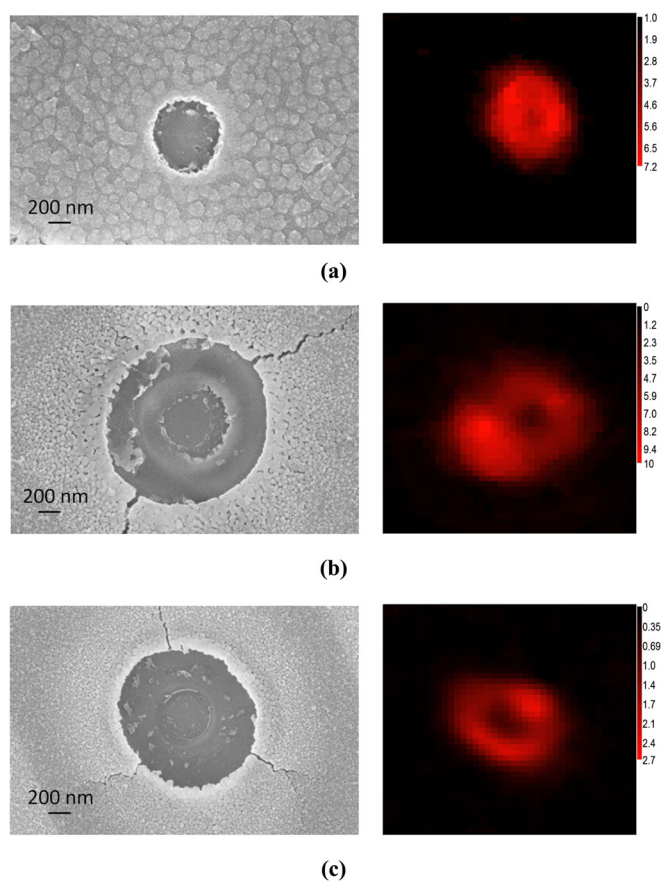


FIG. 4. SEM micrographs of laser-induced graphene from 3 C-SiC and corresponding Raman mapping images: (a) sample A, (b) sample B, and (c) sample C. Raman mapping range is  $4 \mu\text{m} \times 4 \mu\text{m}$  with a spectral range of  $2650\text{--}2750 \text{ cm}^{-1}$ .

<sup>1</sup>K. S. Novoselov, A. K. Geim, S. V. Morozov, D. Jiang, Y. Zhang, S. V. Dubonos, I. V. Grigorieva, and A. A. Firsov, *Science* **306**, 666 (2004).

<sup>2</sup>L. M. Viculis, J. J. Mack, and R. B. Kaner, *Science* **299**, 1361 (2003).

<sup>3</sup>K. S. Kim, Y. Zhao, H. Jang, S. Y. Lee, J. M. Kim, J. H. Ahn, P. Kim, J. Y. Choi, and B. H. Hong, *Nature* **457**, 706 (2009).

<sup>4</sup>X. S. Li, W. W. Cai, J. H. An, S. Y. Kim, J. H. Nah, D. G. Yang, R. Piner, A. Velamakanni, I. H. Jung, E. Tutuc, S. K. Banerjee, L. Colombo, and R. S. Ruoff, *Science* **324**, 1312 (2009).

<sup>5</sup>W. A. de Heer, C. Berger, X. S. Wu, P. N. First, E. H. Conrad, X. B. Li, T. B. Li, M. Sprinkle, J. Hass, M. L. Sadowski, M. Potemski, and G. Martinez, *Solid State Commun.* **143**, 92 (2007).

<sup>6</sup>Y. Zhou and K. P. Loh, *Adv. Mater.* **22**, 3615 (2010).

<sup>7</sup>B. Luo, S. Liu, and L. Zhi, *Small* **8**, 630 (2012).

<sup>8</sup>N. Yue, Y. Zhang, and R. Tsu, *MRS Proc.* **1407** (2012).

<sup>9</sup>S. Lee, M. F. Toney, W. Ko, J. C. Randel, H. J. Jung, K. Munakata, J. Lu, T. H. Geballe, M. R. Beasley, R. S. Hari, C. Manoharan, and A. Salleo, *ACS Nano* **4**, 7524 (2010).

<sup>10</sup>M. G. Lemaitre, S. Tongay, X. Wang, D. K. Venkatchalam, J. Fridmann, B. P. Gila, A. F. Hebard, F. Ren, R. G. Elliman, and B. R. Appleton, *Appl. Phys. Lett.* **100**, 193105 (2012).

<sup>11</sup>M. F. El-Kady, V. Strong, S. Dubin, and R. B. Kaner, *Science* **335**, 1326 (2012).

<sup>12</sup>D. Perrone, G. Maccioni, A. Chiolerio, C. Martinez de Marigorta, M. Naretto, P. Pandolfi, P. Martino, C. Ricciardi, A. Chiodoni, E. Celasco,

- L. Scaltrito, and S. Ferrero, in *Proc. 5th Inter. WLT-Conf. on Lasers in Manufacturing*, Munich, 2009.
- <sup>13</sup>S. N. Yannopoulos, A. Siokou, N. K. Nasikas, V. Dracopoulos, F. Ravani, and G. N. Papatheodorou, *Adv. Funct. Mater.* **22**, 113 (2012).
- <sup>14</sup>J. B. Park, W. Xiong, Y. Gao, M. Qian, and Z. Q. Xie, *Appl. Phys. Lett.* **98**, 123109 (2011).
- <sup>15</sup>D. Wei and X. Xu, *Appl. Phys. Lett.* **100**, 023110 (2012).
- <sup>16</sup>D. Du, Y. Yang, and Y. Lin, *MRS Bull.* **37**, 1290 (2012).
- <sup>17</sup>O. L. Berman and R. Kezerashvili, *J. Phys.: Condens. Matter* **24**, 015305 (2012).
- <sup>18</sup>L. Ju, B. Geng, J. Horng, C. Girit, M. Martin, Z. Hao, H. A. Bechtel, X. Liang, A. Zettl, Y. R. Shen, and F. Wang, *Nat. Nanotechnol.* **6**, 630 (2011).
- <sup>19</sup>H. Da and C. W. Qiu, *Appl. Phys. Lett.* **100**, 241106 (2012).
- <sup>20</sup>A. V. Hamza, M. Balooch, and M. Moalem, *Surf. Sci.* **317**, L1129 (1994).
- <sup>21</sup>J. C. Li, P. Batoni, and R. Tsu, *Thin Solid Films* **518**, 1658 (2010).
- <sup>22</sup>R. Tsu and J. G. Hernandez, *Appl. Phys. Lett.* **41**, 1016 (1982).
- <sup>23</sup>A. Brioude, P. Vincent, C. Journet, J. C. Plenet, and S. T. Purcell, *Appl. Surf. Sci.* **221**, 4 (2004).
- <sup>24</sup>A. C. Ferrari, J. C. Meyer, V. Scardaci, C. Casiraghi, M. Lazzeri, F. Mauri, S. Piscanec, D. Jiang, K. S. Novoselov, S. Roth, and A. K. Geim, *Phys. Rev. Lett.* **97**, 187401 (2006).
- <sup>25</sup>Y. Ohkawara, T. Shinada, Y. Fukada, S. Ohshio, and H. Saitoh, *J. Mater. Sci.* **38**, 2447 (2003).
- <sup>26</sup>A. C. Ferrari, *Solid State Commun.* **143**, 47 (2007).
- <sup>27</sup>G. E. Bacon, *Acta Cryst.* **4**, 558 (1951).
- <sup>28</sup>Y. Zhang and R. Tsu, *Nanoscale Res. Lett.* **5**, 805 (2010).